Liquid-Liquid Phase Behavior of Binary Solutions at Elevated Pressures

JACK WINNICK and J. E. POWERS
University of Oklahoma, Norman, Oklahoma

Isothermal pressure elevation can sometimes cause liquid-liquid phase separation of binary liquid mixtures. A quantitative thermodynamic analysis of this effect is made and applied to the system acetone—carbon disulfide at 0°C. with the use of available P-V-T-X data and vapor pressure data at low pressure. Visual observations of the phase separations at pressures up to 80,000 lb./sq.in. were used to compare with the results of the thermodynamic analysis.

The separation of two liquid phases in equilibrium has been the subject of much study (*1*), and thus the phase behavior of a large number of binary liquid systems has been examined. While both temperature and pressure affect the phase behavior of such systems, few of the investigations have been concerned with the pressure effect (*2*). Correspondingly, the prediction of the effect of pressure on liquid-liquid phase behavior has received almost no attention whatever (*3*).

Timmermans (*4*) was among the first to investigate experimentally the effect of pressure on the mutual solubility of binary liquid mixtures. Subsequent studies of this type have been recently catalogued by Timmermans in a rather comprehensive fashion (*2*).

The general techniques for the use of thermodynamics in the prediction of the effect of pressure on phase equilibria were elucidated over 30 yr. ago by Adams (*5*), and have been used to predict isothermal phase diagrams of solid eutectic forming systems (*5, 6*) and the isothermal solid-liquid phase behavior of binary systems which form solid solutions (*7*). There has, however, been no attempt to use these techniques for the prediction of the pressure effect on the mutual solubilities of liquid pairs.

The thermodynamic prediction of the pressure effect on phase equilibria is invariably dependent on knowledge of solution behavior data for the system in question at some reference pressure as well as the volumetric properties of the phases as functions of pressure (*5*). Solution behavior data, usually expressed in terms of activities, have been the object of a large amount of research, especially for binary mixtures of nonelectrolytes (*2*). The volumetric properties of condensed phases under pressure have not been nearly as well investigated (*8*).

It was decided to develop a method for predicting the effect of pressure on the liquid-liquid phase behavior of a binary mixture of nonelectrolytes. Such a method would be based on thermodynamic relations similar to those developed by Adams (*5, 6*) and by Winnick and Powers (*7*) for solid-liquid behavior. The visual observation of phase separation would also be attempted for comparison with the predicted results.

THERMODYNAMIC DEVELOPMENT

At constant pressure and temperature the criterion for equilibrium in any system is that the Gibbs free energy must be at a minimum (*9*). Thus, a binary liquid system will separate into two liquid phases only if such a configuration will provide the system with a lower free energy than would be available if the system remained as a single phase. It remains only to provide a relationship which will allow the calculation of the free energy of such a system in terms of thermodynamic quantities which are either available or obtainable in the laboratory.

The molal free energy of mixing ΔG^m is defined as the difference between the free energy of a mole of solution and the sum of the free energies of the unmixed components:

$$[\Delta G^m = G_m - \Sigma X_i G_i]_{T,P} \tag{1}$$

Alternatively, this expression can be written as the sum of the ideal and excess free energies of mixing. For the case of a binary mixture

$$(\Delta G^m)_{T,P} = RT\,(X_1 \ln X_1 + X_2 \ln X_2) + (\Delta G^E)_{T,P} \tag{2}$$

True Free Energy Diagram

When plotted against mole fraction, the change in free energy on mixing will appear similar to the lower curve in Figure 1 if substances 1 and 2 are completely miscible. If instead a plot such as the upper curve is obtained, a miscibility gap is indicated. Any mixture whose homogeneous* concentration lies between X_1' and X_1'', say at X_1°,

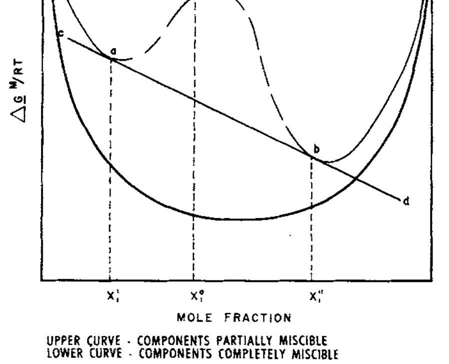

Fig. 1. Hypothetical free energy diagram.

---

* That concentration which would result if the mixture were a single phase.

Jack Winnick is at the University of Missouri, Columbia, Missouri. J. E. Powers is at the University of Michigan, Ann Arbor, Michigan.

will be in equilibrium only when two liquid phases of compositions X_1' and X_1'' are present. Points *a* and *b* are determined from the points of tangency of a straight line *cd*. In this composition range the free energy of two such phases is lower than that resulting from a single phase. The portion of the curve between *a* and *b* is dotted because this is a hypothetical region.

It is easily shown that the concentrations of the phases in equilibrium are determined by a straight line drawn tangent to the curve at two points (*10*) and that the true portion of the curve between these two concentrations is this same straight line (*10*). The reasons for general use of the continuous curve are given by Rowlinson (*11*) and will not be dealt with here.

Effect of Pressure

The effect of external pressure on the free energy of mixing of a binary liquid system can be described as

$$\left(\frac{\Delta G^m}{RT}\right)_{T,P,X} = \left(\frac{\Delta G^m}{RT}\right)_{T,P_o,X} + \frac{1}{RT}\int_{P_o}^{P}\left(\frac{\partial \Delta G^m}{\partial P}\right)_{T,X} dP \qquad (3)$$

From basic thermodynamics

$$\left(\frac{\partial \Delta G^m}{\partial P}\right)_{T,X} = \Delta V^m \qquad (4)$$

so that

$$\left(\frac{\Delta G^m}{RT}\right)_{T,P,X} = \left(\frac{\Delta G^m}{RT}\right)_{T,P_o,X} + \frac{1}{RT}\int_{P_o}^{P} \Delta V^m \, dP \qquad (5)$$

A similar form is obtained in terms of the excess free energy on mixing

$$\left(\frac{\Delta G^E}{RT}\right)_{T,P,X} = \left(\frac{\Delta G^E}{RT}\right)_{T,P_o,X} + \frac{1}{RT}\int_{P_o}^{P} \Delta V^m \, dP \qquad (6)$$

By use of Equation (5), the free energy of mixing for any binary system can be evaluated at any pressure if the free energy is known at some pressure P_o and change in volume on mixing data are available from pressure P_o to the pressure desired over the entire range of composition. If the system in question is completely miscible at pressure P_o, but becomes partially immiscible upon application of pressure, this effect will be indicated by a straight line portion in the free energy diagram as explained above (see Figure 1). Equation (5) indicates this will be possible only if ΔV^m is positive.

Representation of Free Energy Diagram

The free energy curve, or excess free energy curve, at any pressure must be thermodynamically consistent across the range of mole fraction. This consistency can be assured when two sets of data are added, as suggested by Equations (5) and (6), by smoothing with respect to mole fraction using the technique reported by Myers and Scott (*12*). This method utilizes the least-square fitting of the values found from Equation (6) in the form:

$$\left(\frac{\Delta G^E}{RT}\right) = \frac{X_1 X_2}{1 - B(1 - 2X_1)} \sum_{n=0}^{m} A_n (1 - 2X_1)^n \qquad (7)$$

This technique, while not "improving" the data, offers a convenient, thermodynamically consistent means of representing them.

CHOICE OF SYSTEM AND TEMPERATURE

Use of the qualitative tools presented by Prigogine (3) is a great aid in the selection of systems which may separate into two liquid phases under isothermally increasing pressures. Four criteria were used in selecting a system for experimental study (*10*):

1. The system must be a binary nonelectrolyte solution.
2. It must either have been noted to separate under isothermally increasing pressures, or be expected to do so as a consequence of a large positive excess free energy of mixing at 1 atm., and positive volume changes on mixing.
3. Solidification must not occur at pressures below those necessary to cause liquid-liquid phase separation.*
4. The free energy at 1 atm. must be accurately known at a temperature where phase separation can be induced with pressures within the range of the experimental equipment (90,000 lb./sq.in.).

A large number of systems was considered and on the basis of these criteria the system acetone–carbon disulfide was selected for study. The choice was made, in part, because accurate free energy data for this system can be calculated from vapor pressure data which are available at low pressure where the solutions are completely miscible (13). These data are reported at 35.17°C. and it was desirable to make use of these data directly by obtaining volumetric data (*8*) and by observing phase separations at this same temperature. However, preliminary experiments (*10*) revealed that separation into two liquid phases could not be achieved at pressures below the maximum safe pressure of the visual equipment unless the temperature were lowered to 0°C. Therefore volumetric data for the acetone–carbon disulfide system were obtained at 0°C. and the free energy data were adjusted from 35.17° to 0°C. by utilizing additional published data as is described in a later section.

After a complete set of volumetric data had been obtained (*8*) at 0°C., it was decided to make visual observations of phase separations at −2°C. to permit determinations to be made over a wider range of compositions than would have been possible at 0°C. The procedure

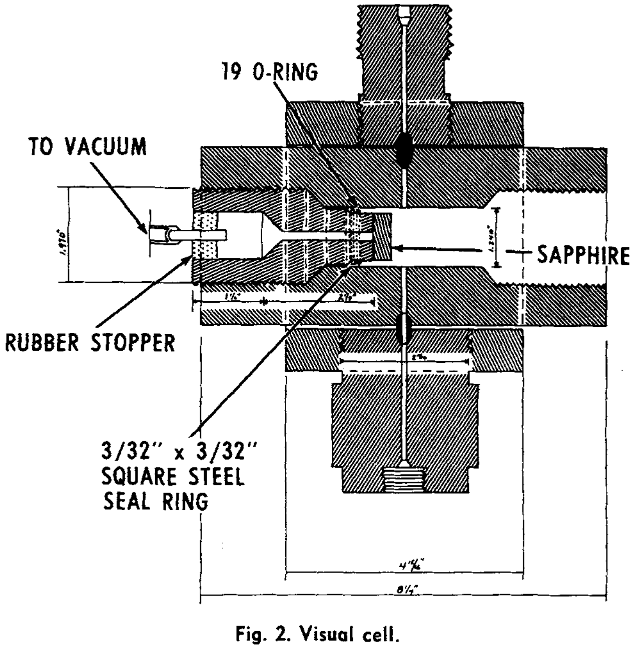

Fig. 2. Visual cell.

---

* Relations which allow the prediction of solidification of a binary system under pressure have been reported by Adams (5) for eutectic forming mixtures and by Winnick and Powers (7) for solid-solution forming mixtures. Such predictions are, however, dependent on knowledge of the behavior of the solid phase under pressure. These data are at present extremely scarce.

used to adjust the phase diagram from −2°C. to 0°C. is described in a later section.

EXPERIMENT

Equipment

Visual Cell. The visual observation cell as shown in Figure 2 is constructed of 4340 steel hardened to about 40 Rockwell C. The cell body is 10 in. long by 4 in. in diameter. The two end plugs are 3½ in. long by 2 in. in diameter. The maximum safe pressure for the cell is 90,000 lb./sq.in. Two 1/32 in. holes lying on a diameter of the cell midway along its length allow access to the cell interior. The yoke, as pictured with its driving plugs, holds two double-ended cones of 5/16 in. tubing firmly in these holes. Replacement of the top coned tubing with a solid double-ended cone resulted in a dead end seal.

The two transparent sapphire windows, which permit visual observation of the experimental mixture in the center of the cell, are 1 in. in diameter by 0.4 in. thick. The pressure seal is made similar to that reported by Poulter (*14*), where the window is sealed against the face of the end plug using the unsupported area principle of Bridgman (*15*). Sealing between the end plug and cell is made by a soft steel ring of square cross section which under an applied load, rides up the 45 deg. angle of the end plug and firmly into the cell. In order to seal securely the window to the end plug, both had to be nearly optically flat. The end plugs were first lapped flat by hand using No. 900 wet grit and then polished with No. 3/0 emery polishing paper. However, because the sapphires were found to be dish-shaped to about five wavelengths from flatness, a good seal was not obtained until some pressure was applied to the chamber. For this reason, a vacuum was applied to the rear of the windows whenever there was no pressure inside the cell. A silicone rubber O-ring, as shown in Figure 2 provided an initial seal between the end plug and cell until a pressure high enough to deform the steel ring was obtained.

The temperature of the cell was maintained by circulating water-glycol solution controlled to ±0.2 F. (*8*) through a copper coil soldered to the cell yoke. About 20 ft. of ¼ in. tubing was used. The coil was covered with Fiberglas insulation held down with heavy-duty cloth-backed tape.

Auxiliary Equipment. The pressure transmission apparatus, gauges, and temperature control have been described elsewhere (*8*). One new piece of equipment was used in this study, other than the visual cell.

To prevent contamination of the sample in the visual observation cell by the pressure transmission fluid (JP-4 jet fuel) an intermediate pressure transmitter had to be used which would act to deliver the pressure into the cell yet not mix with the sample. Mercury was chosen to fulfill this duty. A simple reservoir (*10*) was constructed to contain about 10 cc. Hg and thus keep the JP-4 from reaching the lowest point in the line connected to the optical cell (see Figure 3). If this occurred, the JP-4 would rise above the remaining column of mercury and contaminate the sample under observation.

Procedure

The visual observation cell is shown in Figure 2. Before assembly all parts of the cell were thoroughly cleaned with acetone. The faces of the end plugs were scrupulously cleaned and wiped dry with lens tissue until no dust was apparent. The sapphires were then pressed on firmly. When the interference pattern caused by the air space between sapphire and end plug ceased to change when hand pressure was removed, the sapphire was assumed to be in place. At this time, vigorous shaking would not dislodge the sapphire. A vacuum was applied behind both sapphires to assure that they remained in position. The steel rings were then set in place and the silicone rubber O rings were slipped on above them. The cell was set into position in the yoke and the bottom driving plug and cone were threaded in until the cell was firmly pressed against the top underside of the yoke. This arrangement made a temporary seal at the bottom so that the liquid sample could be inserted. The end plugs were then carefully inserted after all threads were coated with molybdenum-disulfide grease. The vacuum was maintained behind the sapphires at all times (see Figure 2). The mercury leg and reservoir were cleaned with acetone, filled with mercury, and placed in position. The first liquid sample was then injected with a hypodermic syringe and a length of 0.5 mm. I.D. stainless steel tubing. The top cone and driving plug were screwed in tightly using a 16 in. smooth-jawed wrench. Because carbon disulfide attacks all known elastomer O rings, including silicone rubber, the pressure was raised rather rapidly so as to set the steel rings before the O rings dissolved enough to fail; about 60,000 lb./sq.in. was sufficient. The pressure was then slowly released and the sample left in for 24 hr. to allow it to dissolve out as much of the O rings as possible, and thus prevent contamination of subsequent samples. The cell was then drained and the procedure repeated. Rinsing was carried out with acetone, using the hypodermic syringe and tubing, and the experimental trials begun. As long as the end plugs were not moved, the steel rings provided a seal over the entire pressure range. If, however, they had to be removed, the entire sealing procedure had to be repeated with new steel and rubber rings. On removal, the O rings were found to be ragged, soft, and rather lifeless. On immersion in carbon disulfide no further dissolution was apparent.*

Each experimental sample was prepared according to the method of Powers (*16*). The sample was inserted in the same manner as the first and the pressure raised to about 20,000 lb./sq.in. After Fiberglas insulation was wrapped around the cell, cooling was begun and about 12 hr. were allowed to assume thermal equilibrium. The vacuum was removed from behind the sapphires and a mercury-in-glass thermometer was placed into one end plug with its bulb resting against the sapphire, a rubber stopper at the outer end of the plug acting as an insulator. The temperature read on the thermometer

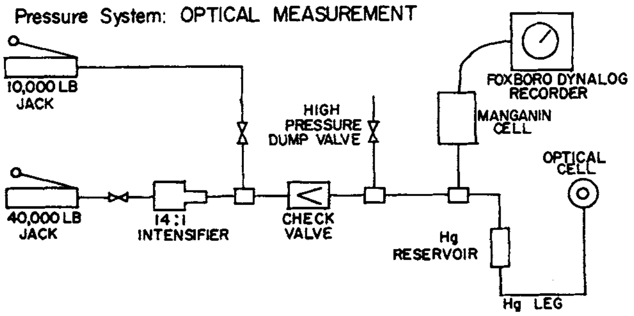

Fig. 3. Experimental equipment.

TABLE 1. OBSERVATION LIQUID-LIQUID SEPARATIONS

Acetone-carbon disulfide

X_1	T, °C.	P, lb./sq. in.
0.1479	−2.0	>82,000*
0.2022	−2.0	76,000
0.2022	−1.75	75,500
0.2494	−2.0	72,500
0.2971	−2.0	73,600
0.2971	−1.0	76,000
0.40	−7.0	64,000
0.40	−2.0	73,000
0.4717	−2.0	74,500
0.5267	−2.0	78,000
0.5267	−1.25	79,500
0.6422	−2.0	>85,000*
0.93	−2.0	>77,500*

* No separation was noted to this pressure.

---

* The O rings were left in a beaker of carbon disulfide for about 1 hr. and removed, the carbon disulfide then being allowed to evaporate. At dryness, no residue was noted. When the same experiment was carried out with a new silicone O ring, a visible film of sediment was observed.

was essentially the same* as that of a copper-constantan thermocouple lying between the yoke and cell. The pressure was increased until cloudiness occurred. It was held there and the temperature allowed to restabilize. The pressure was then lowered until the solution cleared, and then raised again to the translucent pressure. These two pressures, that necessary to cause cloudiness and that to cause clearing, coincided within about 500 lb./sq.in.

That no JP-4 entered the cell during the successful experimental trials was known on the basis of two observations. First, at all times there was a slight leak at the fitting at the bottom of the mercury reservoir. As long as mercury was leaking, it could be safely assumed that no JP-4 could reach the cell. If JP-4 were leaking, it was possible that the column of JP-4 had reached the low point in the mercury leg and could rise into the cell. Second, when JP-4 did enter the cell it was evidenced by streams of high viscosity having an index of refraction much different from the experimental mixtures.

Nine mixtures ranging in composition from 14.79 to 93% acetone were examined at -2°C. As mentioned earlier, this temperature was used instead of 0°C., where the P-V-X and density measurements were made (*8*) in order to obtain a more complete phase diagram. This was the case since the range of pressures where separation occurred was uncomfortably near the limit of the equipment. In order to estimate the effect of temperature on the separation pressure, three samples were allowed to warm slightly, while the pressure was raised sufficient to maintain cloudiness.

At the conclusion of each trial, the cell was warmed by pumping 30°C. water through the copper tubing to prevent any water from condensing inside the pressure chamber during the time the cell was open for rinsing and sample insertion.

Results

The results of the visual observations are listed in Table 1. The resultant curve at -2°C. is shown as Figure 4. Detailed results can be obtained from the junior author.

PREDICTION OF PHASE SEPARATION

To make a prediction of the isothermal liquid-liquid phase diagram to compare with the observed results, Equation (5) must be evaluated over the entire range of composition at every pressure deemed necessary. This requires first that the free energy of mixing curve at atmospheric pressure be established, and second that the integral term involving the change in volume on mixing be evaluated at each pressure.

Free Energy at 1 Atm.

The excellent vapor-pressure data of Zawidsky (*13*) for the system acetone–carbon disulfide at 35.17°C. were used to evaluate the excess free energy of mixing at this temperature. These values were then smoothed with Equation (7). A fourth-order fit was found to represent the data best. The values of the coefficients A_n of Equation (7) are listed as the first row in Table 2. In order to convert the data to 0°C., the enthalpy of mixing data at 16°C. of Schmidt (*17*) and specific heat data at 20°, 30°, and 40°C. of Staveley (*18*) were used in the thermodynamic relation (*10*):

$$\left[\left(\frac{\Delta G^E}{RT}\right)_{0^\circ\text{C.}} - \left(\frac{\Delta G^E}{RT}\right)_{35.17^\circ\text{C.}} = \int_{308.17^\circ\text{K.}}^{273^\circ\text{K.}} \left\{\frac{\Delta H^m{}_{289^\circ\text{K.}} + (\Delta \bar{C}_P{}^m)(T-289)}{RT^2}\right\} dT\right]_X \qquad (8)$$

at each 0.02 mole fraction increment. The resulting values of the difference in the excess free energy on mixing at the two temperatures were smoothed with Equation (7) once more. A third-order fit was sufficient. The resulting constants were $A_0 = -0.277$, $A_1 = -0.089$, $A_2 = -0.080$, and $A_3 = -0.196$.

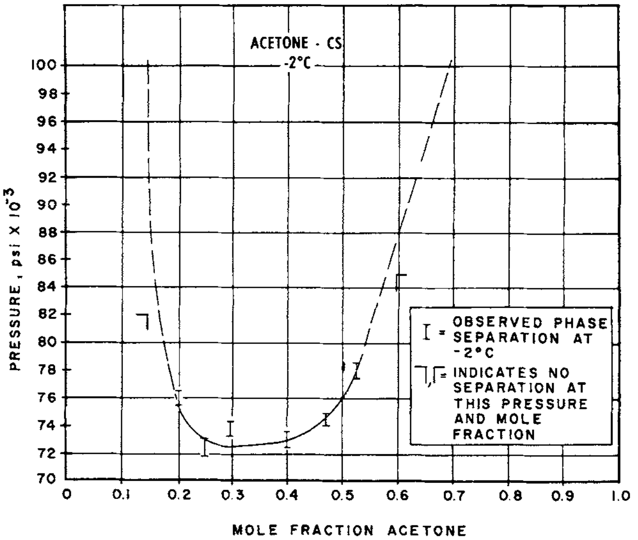

Fig. 4. Observed phase separations.

Unfortunately, two or three of the enthalpy data are inconsistent, as seen in Figure 5. Any error introduced in fitting these data is magnified enormously when used to determine the slope of the free energy curve.

The excess free energy of mixing at 0°C. and 1 atm. was also smoothed with Equation (7). The resultant constants are shown as row 2 of Table 2.

Change in Volume on Mixing

The results for the excess free energy at 0°C. and 1 atm. were used as the basis for calculating the free energy on mixing at each pressure by making use of results reported for the change in volume on mixing for this system at 0°C. (*8*). The change in volume on mixing is represented at any pressure to 100,000 lb./sq.in. and at any mole fraction by

$$\begin{aligned}\Big[\Delta V^m = (\Delta V^m)^o - (V_m)^o \bar{J}_m{}' \ln\left(\frac{\bar{L}_m + P}{\bar{L}_m}\right) \\ + X_1 \,(V_1)^o J_1{}' \ln\left(\frac{L_1 + P}{L_1}\right) \\ + X_2\, (V_2)^o J_2{}' \ln\left(\frac{L_2 + P}{L_2}\right)\Big]_{T,X}\end{aligned} \qquad (9)$$

This relation results from combination of the semiempirical Tait equation for isothermal compressibility with the definition of the change in volume on mixing at any pressure (*8*). The constants $\bar{J}_m{}'$ and $\bar{L}_m$ are independent of pressure but are functions of the composition (*8*):

$$\left.\begin{aligned}\bar{J}_m{}' &= 0.09158 + 0.008499\, X_1 \\ &\quad - 0.03482\, X_1{}^2 + 0.02415\, X_1{}^3 \\ \bar{L}_m &= 17191. - 8455.2\, X_1 \\ &\quad - 131.52\, X_1{}^2 + 4291{,}7\, X_1{}^3\end{aligned}\right\} \quad (10)$$

---

* To within 0.2°C. or as accurately as the thermocouple potential was measured (*10*).

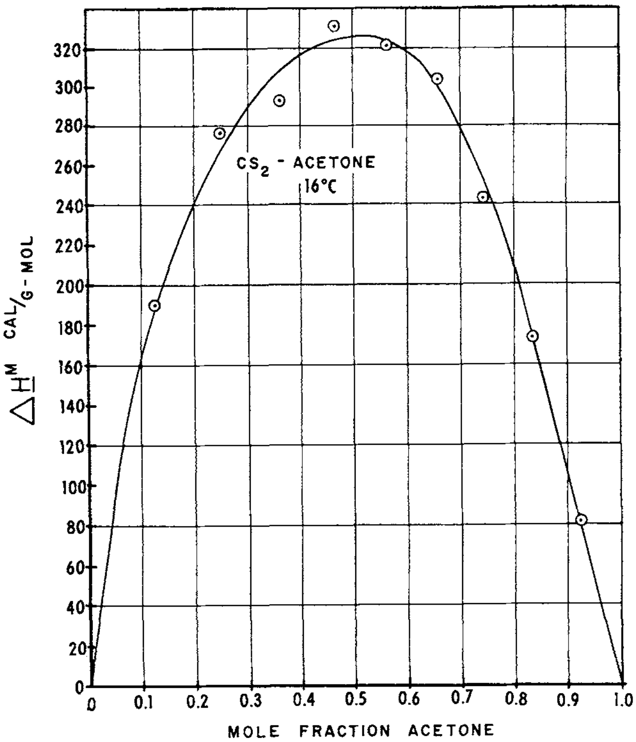

Fig. 5. Reported enthalpy of mixing data (*17*).

The constants J_j' and L_j are evaluated from Equations (10) with $X_1 = 1.0$ for $j = 1$ and $X_1 = 0.0$ for $j = 2$. Equation (9) is integrated to yield

$$\Bigg[\int_{14.7}^{P} \Delta V^m \, dP = P\,(V_m)^o - \bar{J}_m'\,(V_m)^o \left[\bar{L}_m \ln\left(\frac{\bar{L}_m + P}{\bar{L}_m}\right) - P(1 + \ln \bar{L}_m) \right] - \sum_{j=1}^{2} \left\{ X_j (V_j)^o \left[P - J_j' \left(L_j \ln\left\{ \frac{L_j + P}{L_j} \right\} + P \left\{ \ln\left(\frac{L_j + P}{L_j}\right) - 1 \right\} \right) \right] \right\} \Bigg]_{T,X} \tag{11}$$

Table 2. Results of Smoothing $\Delta G^E/RT$

T, °C.	P, lb./sq.in.	A_0	A_1	A_2	A_3	A_4
35.17	14.7	1.600	0.896	0.158	0.127	0.439
0	14.7	1.877	0.985	0.238	0.323	0.439
0	10,000.0	1.979	1.016	0.252	0.301	0.453
0	20,000.0	2.061	1.043	0.268	0.280	0.466
0	30,000.0	2.132	1.064	0.283	0.259	0.478
0	40,000.0	2.196	1.081	0.298	0.239	0.490
0	50,000.0	2.255	1.093	0.312	0.220	0.501
0	60,000.0	2.310	1.101	0.326	0.201	0.513
0	70,000.0	2.363	1.106	0.338	0.183	0.524
0	80,000.0	2.413	1.108	0.351	0.165	0.535
0	90,000.0	2.461	1.107	0.362	0.148	0.545
0	100,000.0	2.507	1.104	0.373	0.131	0.556

Prediction of Phase Behavior

This integral was evaluated at each 5,000 lb./sq.in. increment in pressure and added to the excess free energy on mixing at 1 atm. and 0°C. as suggested by Equation (6). These results were fitted at each pressure with Equation (7). A fourth-order fit was used, as was for the curves at 1 atm. The equations were converted from excess to total molal free energy change on mixing with Equation (2). The constants representing the excess free energy at each 10,000 lb./sq.in. increment in pressure are listed in Table 2. Values of $\Delta G^m/RT$ thus calculated were plotted vs. composition with a Calcomp plotter. Some representative curves are shown in Figure 6. The straight lines in the figure were drawn by hand and their points of tangency to the curves indicate the compositions of the phases predicted to be in equilibrium. These points are shown plotted as pressure vs. composition in Figure 7.

As noted previously, phase separations were observed experimentally at −2°C., whereas the thermodynamic predictions were made at 0°C. In order to adjust the experimentally observed results (Figure 4) from −2° to 0°C., the variation in pressure of phase separation with temperature was determined for several solutions in the temperature range from −7.0° to −1.0°C. (Table 1). Values of the rate of change of pressure of phase separation with temperature $(\partial P/\partial T)_X$ were estimated from these

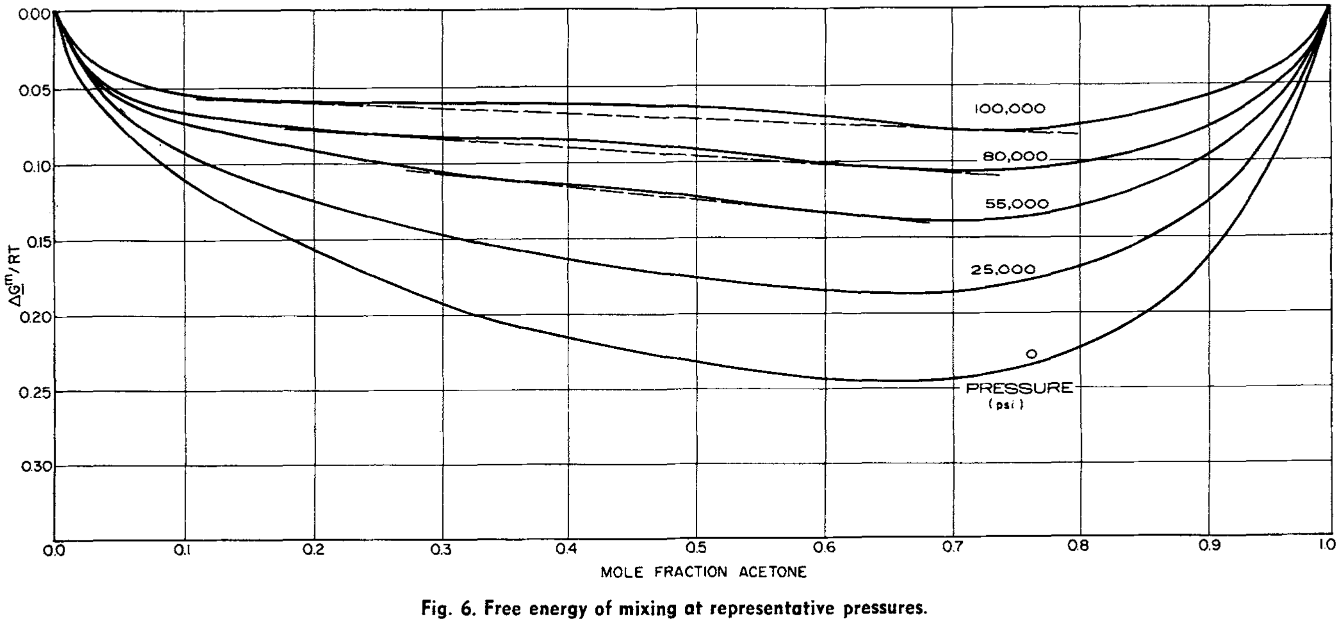

Fig. 6. Free energy of mixing at representative pressures.

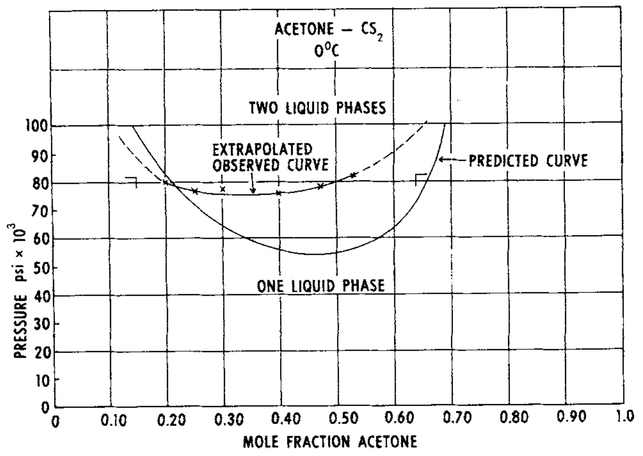

Fig. 7. Comparison of predicted and observed phase diagrams.

results and used to estimate the pressures of phase separation at 0°C. plotted in Figure 7.

CONCLUSIONS

The agreement between the predicted and extrapolated observed curves in Figure 7 is quantitatively less than desirable. There is, however, substantial qualitative agreement. Error analysis carried out on the compressibility measurements indicate the possibility of 1 to 5% error in the change in volume on mixing (*10*). Several other causes undoubtedly contributed to the lack of agreement. In order to make the prediction, the experimental data of three different investigators had to be incorporated: the vapor-pressure data of Zawidsky, the specific heat data of Staveley, and the heat of mixing data of Schmidt. Of these, the last are least reliable. The curve in Figure 5 was taken to be an accurate representation of the experimental data and no adjustment was made to improve the agreement between the predicted and observed results. However, a curve can be drawn through the data of Schmidt (Figure 5) which would yield quantitative agreement between the resulting prediction of phase separation and the results presented in Figure 7. This curve would lie within the limits of accuracy of the reported heat of mixing data.

The extrapolated observed curve is subject to unknown error of extrapolation with a minimum amount of data. In addition, the actual data may be in error due to the errors in temperature and pressure measurements and sample purity. The effect of the last is especially difficult to estimate. The critical solution pressure may be shifted either upward or downward by very small amounts of impurities (*19*).

A study analogous to this one has been reported by Williamson and Scott (*20*). They attempted to match predicted and observed liquid-liquid phase separation for two systems. However, while the present study examines the effect of pressure isothermally, Williamson and Scott examined the effect of temperature isobarically. It is interesting to note that similar relative agreement is reported. The authors mention extreme sensitivity of the prediction to small uncertainties in the excess properties.

The contributions of the present study are summarized as follows:

1. A method has been described which can be used to predict the pressure of isothermal liquid-liquid phase separation making use of free energy data at low pressure and volumetric data over the entire pressure range.
2. A calculational procedure is given that provides a means of checking the thermodynamic consistency of several diverse types of data.
3. The isothermal liquid-liquid phase diagram for the system acetone–carbon disulfide has been determined at −2°C.

ACKNOWLEDGMENT

The authors wish to thank all the members of the faculty of the University of Oklahoma who gave their help at various times during the course of the research.

A special note of thanks is due Professor W. W. Robertson of the Physics Department at the University of Texas for the use of his high pressure cell in making the visual observations.

Many of the calculations were carried out in the computer facilities of the University of Missouri, Columbia, Missouri, and the Oak Ridge National Laboratory, Oak Ridge, Tennessee.

The study was made possible by a grant from the National Science Foundation.

NOTATION

A_n = coefficient in series [Equation (7)]
B = skewing factor [Equation (7)]
$\Delta \bar{C}_p{}^m$ = average molal change in specific heat on mixing
G_i = molal free energy of pure component i
ΔG^E = excess molal change in free energy on mixing
G_m = molal free energy of mixture
ΔG^m = molal change in free energy on mixing
ΔH^m = molal change in enthalpy on mixing
J_1' = Tait equation constant for pure compound 1 [Equation (9)]
J_2' = Tait equation constant for pure compound 2 [Equation (9)]
$\bar{J}_m'$ = best fit value for Tait constant [Equation (9)]
L_1 = Tait equation constant for pure component 1 [Equation (9)]
L_2 = Tait equation constant for pure component 2 [Equation (9)]
$\bar{L}_m$ = best fit value for Tait constant [Equation (9)]
P = pressure, lb./sq. in.
P_o = initial pressure, lb./sq. in.
R = gas constant
T = temperature
$(V_1)^o$ = molal volume of pure component 1 at 1 atm.
$(V_2)^o$ = molal volume of pure component 2 at 1 atm.
$(V_j)^o$ = molal volume of pure component j at 1 atm.
$(V_m)^o$ = molal volume of mixture at 1 atm.
ΔV^m = molal change in volume on mixing at pressure P
$(\Delta V^m)^o$ = molal change in volume on mixing at 1 atm.
X = mole fraction
X_j = mole fraction component j
X_1 = mole fraction component 1 (acetone)
X_2 = mole fraction component 2 (carbon disulfide)
X_1' = mole fraction component 1 in phase 1
X_1'' = mole fraction component 1 in phase 2
X_1^o = hypothetical homogeneous composition (Figure 1)

LITERATURE CITED

1. Alders, L., "Liquid-Liquid Extraction," Elsevier, New York (1955).
2. Timmermans, Jean, "Physico-Chemical Constants of Binary Systems in Concentrated Solutions," Interscience, New York (1959).
3. Prigogine, I., and R. Defay, "Chemical Thermodynamics," p. 289, Longmans-Green, New York (1954).
4. Timmermans, Jean, *J. Chim. Phys.*, **20**, 491 (1923).
5. Adams, L. H., *J. Am. Chem. Soc.*, **53**, 3769 (1931).
6. *Ibid.*, **54**, 2220 (1932).
7. Winnick, Jack, and J. E. Powers, *A.I.Ch.E. J.*, **7**, 303 (1961).
8. *Ibid.*, this issue.
9. Moelwyn-Hughes, E. A., "Physical Chemistry," Pergamon, New York (1957).

10. Winnick, Jack, Ph.D. thesis, Univ. Oklahoma, Norman (1963).
11. Rowlinson, J. S., "Liquids and Liquid Mixtures," p. 136, Butterworth, London (1959).
12. Myers, D. B., and R. L. Scott, *Ind. Eng. Chem.*, **55**, 43 (1963).
13. Zawidzky, J. V., *Z. Phys. Chem.*, **35**, 154 (1900).
14. Poulter, T. C., *Phys. Rev.*, **35**, 297 (1930).
15. Bridgman, P. W., "The Physics of High Pressure," p. 39, Macmillan, New York (1931).
16. Powers, J. E., *Chem. Anal.*, **49**, 54 (1960).
17. Schmidt, G. C., *Z. Phys. Chem.*, **21**, 221 (1926).
18. Staveley, L. A. K., et al., *Trans. Faraday Soc.*, **51**, 323 (1955).
19. Findlay, Alexander, "Phase Rule," p. 101, Dover, New York (1951).
20. Williamson, A. G., and R. L. Scott, *J. Phys. Chem.*, **65**, 275 (1961).

Manuscript received July 23, 1965; revision received November 22, 1965; paper accepted November 23, 1965. Paper presented at A.I.Ch.E. Houston meeting.

Axial Mixing and Extraction in a Mechanically Agitated Liquid Extraction Tower

ROGER E. BIBAUD and ROBERT E. TREYBAL
New York University, New York, New York

Axial mixing was measured in both phases for a countercurrently operated, mechanically agitated extractor of the Oldshue-Rushton design for water continuous and toluene and kerosene dispersed. Results in terms of an eddy axial diffusivity were correlated in terms of the variables studied. These correlations were then applied to column performance during extraction of n-butyl amine from kerosene into water, and the true mass transfer coefficients, corrected for axial mixing, were determined. These are shown to be predictable for droplets of dispersed phase considered to be rigid spheres.

Axial mixing in liquid-extraction towers is the combined effect of two phenomena: that due to turbulent and molecular diffusion in the axial direction and that resulting from a nonuniform velocity across the cross section of the tower. It exists in both the continuous and dispersed liquids. It is undesirable, since the difference between solute concentrations in the two contacted liquids is thereby reduced, in turn resulting in lower rates of extraction than would prevail under plug-flow conditions.

Atttention was first called to the results of axial mixing in extractors around 1950 (*6, 8, 20*) when a substantial *end effect*, in reality an alteration of the plug-flow countercurrent concentration profile attributable to axial mixing, was noted in spray towers. Since then, methods of taking it into account in the design of extractors have been developed (*17, 24*) but these depend upon having at hand experimental measurements of the axial mixing effect, or means of predicting it. Methods of measurement have been reviewed (*15*). Despite the great importance of the phenomenon in liquid extraction, there have been relatively few measurements in equipment of interest under typical extraction conditions, that is, with two liquid phases flowing countercurrently: for the continuous phase in a small column (*11*); the continuous (*15, 23*), dispersed (*2*), and both phases (*18*) in small pulsed columns; both phases in packed columns (*13, 14*); the continuous phase in a reciprocating plate column (*7*); and both phases in rotating disk contactors (RDC) (*25*). There are no published data for two-phase flow in the types of towers used in the present work, although a report was made (*9*) of measurements taken during the flow of water alone.

EDDY DIFFUSIVITY OF AXIAL MIXING

For devices wherein the concentrations of dissolved solute change continuously with axial distance, on the assumption that the axial mixing can be adequately described by an eddy diffusivity E, the material balances over a differential height of the extractor for the raffinate liquid are

---

Roger E. Bibaud is with Vitro Engineering Company, New York, New York.